

NONLINEAR OPTICAL PHENOMENA

https://doi.org/10.1070/QEL18060

Stimulated low-frequency Raman light scattering in systems of nano- and submicron-sized particles

M.A. Karpov, A.D. Kudryavtseva, M.A. Shevchenko, N.V. Tcherniega, S.F. Umanskaya

Abstract. **We present a brief review of experimental work on the investigation of stimulated low-frequency Raman scattering of light in systems of submicron and nanosized particles of various physical nature.**

Keywords: *stimulated low-frequency Raman scattering, nanoparticles, submicron particles.*

1. Introduction

Any spatially limited body, regardless of its size, has a set of acoustic eigenfrequencies, whose values are determined by the size of the body, its elastic characteristics, and the characteristics of the environment. For bodies of submicron size, eigenfrequencies lie in the gigahertz range, and for nanosized bodies (with a characteristic size of less than 100 nm) they are in the terahertz range. Deformation of nanoparticles in an electric field leads to a change in their polarisability [1]. When changing the shape of particles from spherical (with radius R) to spheroidal, the change in polarisability can be represented as

$$\Delta\alpha = \frac{3V(a-b)}{5\pi R} = \frac{4\alpha_0(a-b)}{5R}, \tag{1}$$

where V is the particle volume; a and b are the lengths of the major and minor semiaxes of the spheroid; and a_0 is the polarisability of a spherical particle. A change in the ΔV volume also leads to a change in the polarisability:

$$\Delta\alpha = \frac{\alpha_0 \Delta V}{V}. \tag{2}$$

In view of the possibility of volume and (or) shape variation of a particle in an electromagnetic field, systems of particles with given spatial and elastic characteristics can be used as media with artificially given nonlinearity.

For the first time, the possibility of using the mechanical deformation of particles to obtain the desired nonlinear optical properties was pointed out in Ref. [2]. It considered the feasibility of using media with induced deformation, primarily for studying the mechanism of self-focusing. Fluctuations in the shape of a liquid droplet were theoretically studied in Ref. [3], where it was shown that the thermal vibrations of a liquid droplet accompanied with a change in shape can lead to inelastic light scattering from the droplet. The mechanism of inelastic scattering by a droplet was considered by analogy with molecular Raman scattering of light. It was assumed that a droplet in an external electromagnetic field (provided that its size is much smaller than the wavelength of electromagnetic radiation) is polarised, acquiring a dipole moment that oscillates in time with the frequency of the thermal vibration. As a result, the re-emission spectrum contains components that are shifted with respect to the exciting radiation by the eigenfrequency of acoustic vibrations of the droplet. For the first time, inelastic light scattering by acoustic vibrations of solid nanosized particles was observed experimentally in 1986 [4]. This process is analogous to spontaneous Raman scattering (RS) of light by molecular vibrations. The difference lies in the frequency shift, which for such an RS is much greater than in the case of light scattering by natural acoustic vibrations of nanosized and submicron particles.

In the modern scientific literature, the inelastic light scattering by acoustic vibrations of nanosized and submicron particles of various shapes is called 'spontaneous low-frequency Raman scattering (LFRS) of light'. To describe the vibrations of solid particles, advantage is taken, as a rule, of the approach developed by Lamb [5] or, in the case of liquid nanosized (submicron) particles, of the Flügge model [6], which was applied to problems of the droplet nuclear model. The vibrational dynamics of spherical particles, which determines the frequency shift of the LFRS radiation, was studied in sufficient detail by Lamb [5], who considered the vibration of a free homogeneous sphere of arbitrary size and determined the vibrational modes arising in this process. Note that the Lamb approach can be used to estimate the vibration frequencies of objects of different sizes. Using this approach, one can calculate the parameters of vibrational modes of spherical objects of different sizes, from planets to nanoparticles. These modes are classified as torsion and spheroidal, described by the orbital quantum number l and the harmonic number. The experimentally obtained values of the eigenfrequencies of particle vibrations in most works agree with the frequencies calculated by the method developed by Lamb, in which the particle surface is assumed to be free. As a rule, nanoparticles are not free under real conditions.

M.A. Karpov, A.D. Kudryavtseva, M.A. Shevchenko, N.V. Tcherniega, S.F. Umanskaya P.N. Lebedev Physical Institute, Russian Academy of Sciences, Leninsky prosp. 53, 119991 Moscow, Russia;
e-mail: kudryavcevaad@lebedev.ru

Received 23 January 2022; revision received 13 February 2022
Kvantovaya Elektronika **52** (6) 580–586 (2022)
Translated by by E.N. Ragozin

In a number of cases, especially when the Lame constants and the particle and matrix densities differ insignificantly, it is necessary to take into account the influence of the medium surrounding the particle. Localised acoustic phonons in nanosystems are mechanical vibrations with a frequency on the order of the ratio of the sound speed in the medium to the size of the object. For a particle in a solid matrix, vibrations gradually decay due to the emission of sound waves into the surrounding matrix. The problem of finding eigenfrequencies for a solid sphere surrounded by an infinite continuous medium was first solved by Dubrovskii [7] as applied to vibrations of a rigid body. The frequency values obtained in this work are complex, their imaginary part being related to the damping of vibrations. To carry out the calculations, it is necessary to know the values of the densities and speeds of sound for the matrix and the particle inside it. This approach is used to calculate the frequency values with the inclusion of the influence of the matrix.

Of great interest is the study of acoustic excitations in suspensions, i.e., of solid particles contained in a liquid. The case of a nanoparticle in a liquid can be considered as a special case of the solution obtained by Dubrovskii, taking into account the zero transverse sound velocity in the liquid, which was done in Ref. [8]. However, the viscosity of the liquid, which has a significant effect on the vibrations of the particle, is neglected in this case. In a number of works, viscosity was taken into account only for torsional vibrational modes of biological structures. Note that the viscosity of the medium significantly affects the vibrations of objects whose dimensions do not exceed 100 nm. For larger sizes, the effect of viscosity can be neglected. Using the generally accepted terminology, it can be argued that this effect should be taken into account for nanosized particles, but not for submicron particles.

Not all vibrational modes will show up in the LFRS spectrum. On the basis of group theory, it was shown [9] that only spheroidal modes with $l = 0$ (radial) and $l = 2$ (quadrupole) are Raman-active. However, this is true for spherical particles with sizes much smaller than the wavelength and larger than a few nanometres, when the discreteness of the crystal lattice can still be ignored. With an increase in the particle size, the appearance of anisotropy, and also with the deviation of the shape from the spherical one, modes with different l can become Raman-active. Note that the radial mode ($l = 0$) is completely polarised, while the quadrupole mode ($l = 2$) is depolarised.

The physical mechanism of the photon–phonon interaction depends on the system and determines the relative activity of the two types of vibrations. For metal particles, vibrational modes with $l = 2$ dominate the Raman spectrum. For dielectric particles, both quadrupole and radial modes can appear in the spectra, depending on which particular mechanism of photon–phonon interaction prevails. The LFRS intensity depends on the microscopic structure and the physical mechanism of the photon–phonon interaction, which modulates the polarisability. These mechanisms can be different for semiconductor, metallic, and dielectric particles [10–13].

We note the connection of LFRS with other types of light scattering. Inelastic types of scattering are well known, which are caused by the interaction of electromagnetic radiation with vibrations of individual molecules (RS) and a system of bound molecules, or an acoustic phonon [Brillouin scattering (BS)]. Both processes can be considered as a parametric interaction of waves and at the same time have a number of distinctive features. The spectral shifts in these processes are in different ranges, and therefore different types of experimental equipment are used to record them. For the spontaneous mode in RS, the frequency does not depend on the direction of the wave vector, in contrast to the BS. Furthermore, for the stimulated regime, in the case of stimulated Brillouin scattering (SBS), scattering in the direction of pump propagation does not occur.

The interaction of electromagnetic radiation with spatially limited systems in the form of mesoscopic particles of various shapes and different physical nature, leading to inelastic scattering by the natural acoustic vibrations of particles (LFRS), is a process that is at the junction of these types of scattering. Changing the ratio between the wavelength of the incident radiation and the size of the particle leads to a transition from one type of scattering to another, when different physical processes are involved in the scattering mechanism.

For small particles whose sizes are much smaller than the wavelength, scattering arises due to a change in polarisability, similar to how it occurs in the Raman scattering. There is no dependence on the direction of the wave vector. This mechanism is called Raman in the literature on LFRS. When the particle size is comparable to the wavelength of light, scattering due to fluctuations in the density of matter begins to dominate. This mechanism is called the Brillouin mechanism. However, unlike ordinary BS, only the scattering intensity depends on the direction of the wave vector, while the frequency is determined by the particle morphology and remains constant [14].

The parameters of the LFRS spectra (types of excited modes, frequency shift, linewidth) are therefore determined by the properties of the particles themselves, such as size, shape, and physical nature, as well as by the characteristics of the surrounding matrix, which makes this type of scattering effective for studying various properties of nanosized and submicron systems. The specific form of the spectral distribution of the LFRS intensity is determined, in addition to the acoustic properties of the particles, by their size distribution. LFRS can be used to determine not only the acoustic properties, but also the type of size distribution of nanoparticles. The difficulties encountered in experimental studies of LFRS are that the frequency shifts during LFRS are in the giga- and terahertz frequency ranges for submicron and nanosized particles, respectively, and the energy efficiency of the process is very low.

2. Stimulated low-frequency light scattering

As is well known, to any type of spontaneous light scattering there corresponds a stimulated type of scattering. The nonlinear interaction of a strong laser wave with the initially weak seed radiation of spontaneous LFRS can lead to the appearance of stimulated low-frequency Raman scattering (SLFRS) of light. For the first time, SLFRS of light was recorded in synthetic opal matrices, which are three-dimensional fractal-type structures formed from close-packed monodisperse silica globules with a characteristic diameter of 200–700 nm [15, 16]. The presence of photonic band gaps in such structures leads to the appearance of an anomalously high density of photonic states in the corresponding spectral regions and,

as a consequence, to the high efficiency of a number of different nonlinear optical processes [17]. The infiltration of opal matrices with media with a refractive index close to that of quartz makes it possible to obtain nanocomposites that are transparent in the visible region of the spectrum and change the parameters of the photonic band gap.

The setup employed to study the SLFRS is schematised in Fig. 1. The SLFRS was excited by the radiation of a *Q*-switched ruby laser. The laser wavelength is 694.3 nm, the pulse duration is 20 ns, and the width of the oscillation spectrum is 0.015 cm^{-1}. To record the scattered radiation spectrum, Fabry–Perot interferometers were used, and the radiation was recorded both in the opposite ('backward') direction to the pump radiation, and in the ('forward') direction accompanying the pump radiation. In experiments to study forward SLFRS, use was made of nanocomposite samples, which were synthetic opals infiltrated with media with a refractive index close to that of quartz. The detection threshold, the spectral structure of the scattered radiation, and the conversion efficiency were determined. The spectral shift of the first Stokes component with respect to the pump frequency was approximately several tenths of cm^{-1}. This frequency shift is defined by the natural vibration frequency of the silica globules forming the opal matrix. The data of Refs [15, 16] are in good agreement with those obtained in the study of LFRS in synthetic opals [18] and also agree with the results of calculations performed using the Lamb approach. Nanocomposites containing different nonlinear media have been studied. The parameters of the samples, in which the SLFRS was observed, are given in Table 1. The highest pump-to-SLFRS wave conversion efficiency realised in these experiments amounted to 60%.

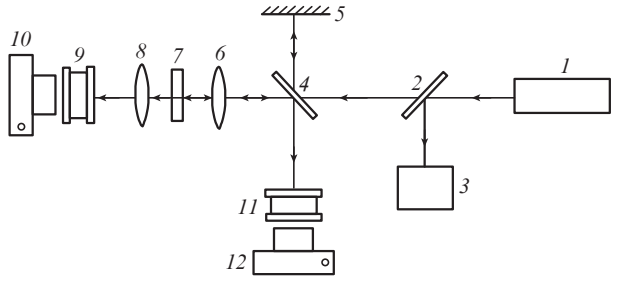

Figure 1. Schematic of the experimental setup:
(1) laser; (*2*, *4*) beam splitters; (*3*) system for recording laser radiation parameters; (*5*) mirror; (*6*, *8*) lenses; (*7*) sample; (*9*, *11*) Fabry–Perot interferometers; (*10*, *12*) interferogram recording systems.

Note that the liquids filling the synthetic opals used in these experiments are Raman-active. However, taking into account the small amount of substance in the samples under study due to the pore volume, stimulated Raman scattering (SRS) was not excited in most samples at the pump intensities used. The exception is the case when the wavelength of the Stokes component falls on the edge of the photonic bandgap. In this case, a high-efficiency SRS was observed. Issues related to the study of the feasibility of controlling the position of the photonic band gap in order to efficiently generate SRS were considered in Ref. [19].

Synthetic opals are ordered structures, in contrast to polycluster films, in some of which SLFRS was also observed.

Table 1. Characteristics of nanocomposites (the ratio of the refractive index of the substance with which the opal matrix was filled to the refractive index of quartz and the diameter of the globules of the synthetic opal samples used), in which SLFRS was observed, and the scattering geometry.

Substance	n/n_{SiO_2}	D/nm	Geometry of realised stimulated scattering
Nitrobenzene $C_6H_5NO_2$	1.07	200	Backward SLFRS
		230	Backward SLFRS
		260	Backward SLFRS
		300	Backward SLFRS, **SRS**
		320	Backward SLFRS
Benzene C_6H_6	1.04	200	Backward SLFRS
		230	Backward SLFRS
		260	Backward SLFRS
		300	Backward SLFRS
		320	Backward SLFRS
Carbon tetrachloride CCl_4	1.01	200	Backward SLFRS
		230	Backward SLFRS
		260	Backward SLFRS
		300	Backward SLFRS
		320	Backward SLFRS
Acetone CH_3COCH_3	0.930	200	Backward and forward SLFRS
		230	Backward and forward SLFRS
		260	Backward and forward SLFRS
		300	Backward SLFRS
		320	Backward and forward SLFRS
Ethanol C_2H_5OH	0.930	200	Backward and forward SLFRS
		230	Backward and forward SLFRS
		260	Backward and forward SLFRS
		300	Backward and forward SLFRS
		320	Backward and forward SLFRS
Water H_2O	0.917	200	Backward and forward SLFRS
		230	Backward and forward SLFRS
		260	Backward and forward SLFRS
		300	Backward SLFRS
		320	Backward and forward SLFRS
Opal SiO_2	0.690	200	Backward SLFRS
		230	Backward SLFRS
		260	Backward SLFRS
		300	Backward SLFRS
		320	Backward SLFRS

Stimulated light scattering caused by the interaction of laser radiation with localised acoustic modes of structural disordered inhomogeneities in solid-state systems was implemented in Ref. [20]. Polycluster diamond films (PDFs), aluminium nitride films (AlNFs), indium tin oxide films (ITFs), as well as regular packings of SiO_2 nanospheres (RPNs) were studied. All these materials can be characterised by the average sizes of structural inhomogeneities, which are determined by the growth conditions. The sizes of inhomogeneities are on the order of several hundred nanometres (from 200 to 1900 nm), which corresponds to acoustic frequencies in the gigahertz range. Table 2 lists the characteristic sizes of film inhomogeneities obtained from electron microscopy data, as well as the spectral shifts of the Stokes components of the SLFRS. SLFRS was observed in all the samples under study, and in a

Table 2. Characteristics of the samples and parameters of the SLFRS implemented with them.

Sample number	Film/ substrate	Stokes component shift/cm^{-1}	Characteristic inhomogeneity size/μm
1	AlN/glass	0.27	0.8
2	AlN/glass	0.20–0.29	0.6–1.2**
3	$InSnO_x$/glass	0.21, 0.25, 0.33	1.8
4	$InSnO_x$/glass	0.29	1.7
5	$InSnO_x$/glass	0.17–0.28*	1.9
6	PCD/diamond	0.34	0.8
7	PCD/diamond	0.26–0.30	0.6–0.9**
8	$RPSiO_2$/glass	0.24	0.25

*Spread of values over a specimen; ** The structure parameters vary with film thickness.

number of samples several Stokes components were recorded (three Stokes components for sample 3 and two Stokes components for sample 2).

Another example of inhomogeneous disordered systems is suspensions of nanosized and submicron particles of various physical nature, including biological ones. The nonlinear optical properties of such systems are currently the subject of intense experimental and theoretical research. The optical properties of dispersed systems are determined both by the physical nature, shape, particle size of the dispersed phase, and by the properties of the liquid phase. The most common methods for studying the optical properties of disperse systems include the use of various types of light scattering, including stimulated scattering. In a heterogeneous medium with a nonuniform distribution of the refractive index, the interaction of electromagnetic field with particles due to electrostriction leads to the appearance of concentration flows. This effect is the cause of stimulated concentration light scattering (SCLS). SCLS in suspensions [21, 22] is an example of a nonlinear optical process typical for systems of nanosized or submicron particles in a liquid matrix. During SCLS there occurs interference of the exciting and scattered waves and an interference intensity grating, in the antinodes (or minima) of which particles of suspension are drawn. Produced as a result is a lattice of particle concentration and, consequently, of the refractive index. SCLS spectroscopy makes it possible to obtain information about the system as a whole, primarily about the concentration of particles. To characterise such systems, information is required both about the system as a whole and about the properties of its constituent particles, for example, about their morphology.

One of a fairly large number of methods for studying suspensions is the LFRS method, which makes it possible to obtain information about the size distribution of particles, their acoustic properties, as well as their size and shape. If such a system is monodisperse, then its interaction with pulsed laser radiation can lead to its coherent acoustic excitation and generation of SLFRS. The advantage of using suspensions is the ease of their preparation, as well as the ability to easily change the concentration and type of solvent. Naturally, the monodispersity of the system determines the pump-to-SLFRS wave conversion efficiency. SLFRS with a high conversion efficiency has been obtained in suspensions of gold and silver nanoparticles [23], zinc sulphide [24], detonation-produced diamonds [25], copper oxide [26], and sodium chloride [27]. In suspensions, SBS may be excited simultaneously with SLFRS. In Ref. [28], SLFRS and SBS were excited in an aqueous suspension of spherical SiO_2 particles with a radius of 150 nm. The experimentally measured spectral characteristics of scattering were in good agreement with the calculated data.

We emphasise the influence of the medium surrounding the particle on the parameters of the SLFRS and LFRS, primarily on the efficiency of these processes, in the case when the acoustic characteristics of the particles and the medium in which they are located are close. This situation, as a rule, takes place in systems of biological particles, including viruses. The study of SLFRS, with the inclusion of the influence of the environment in these systems, was carried out in Refs [29–31]. SLFRS can be used not only as a spectral method to characterise systems of submicron and nanosized particles, but also, taking into account the high conversion efficiency, as a source of biharmonic pumping with a difference frequency in the giga- and terahertz ranges. Such a source can be used for selective and resonant effects on systems that have their own acoustic frequencies that coincide with the difference frequency. This possibility is of greatest interest for systems of biological particles, including viruses. The possibility of using biharmonic pumping for these purposes was discussed in Ref. [32].

The interaction of two-frequency radiation with a system of submicron particles was experimentally demonstrated using a scheme containing two cells [33]. The first cell served as a source of biharmonic pumping; it contained an oil-in-water emulsion (an emulsion of cutting fluid EM-1 in water) with an average oil droplet size of 300 nm. The emulsion was prepared using double distilled water further purified with Superpure PVDF and EM-1 LC filters. Before optical measurements, the emulsion was subjected to ultrasonic stabilisation of parameters. The size distribution of oil droplets (Fig. 2) was obtained by dynamic light scattering technique.

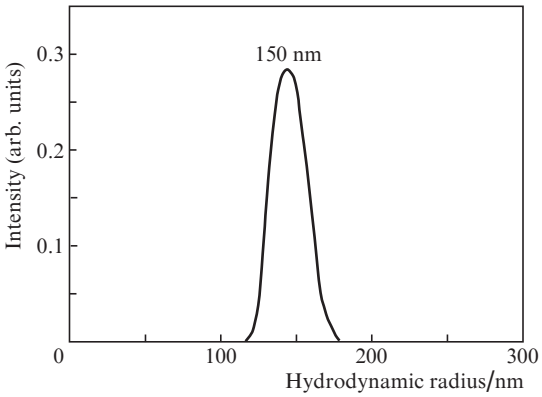

Figure 2. Size distribution of oil droplets.

The SLFRS was excited in the first cell by ruby laser radiation using the setup shown in Fig. 1. The threshold of SLFRS for radiation propagating in the forward and backward directions was ~0.1 GW cm^{-2}. The experimentally measured frequency shift Ω of the first Stokes component was 5.4 GHz for the forward and backward SLFRS. This frequency shift corresponds to the radial vibrations of the oil drop. The highest conversion efficiency of pump radiation into scattered light

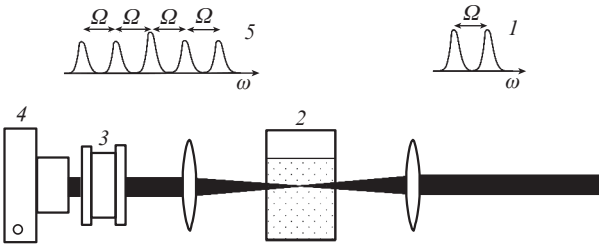

Figure 3. Schematic of the experiment:
(*1*) spectrum of biharmonic pump radiation; (*2*) cell; (*3*) Fabry–Perot interferometer; (4) interferogram recording system; (5) emission spectrum at the output of the cell.

for the given experimental excitation conditions exceeded 60% for forward SLFRS. The schematic of the experiment is shown in Fig.3.

A quartz cell filled with an oil-in-water emulsion was illuminated with biharmonic radiation, which was focused into the centre of the quartz cell by a lens with a focal length of 20 cm. A Fabry–Perot interferometer was used to measure the spectrum of radiation emerging from the cell. During the measurements, the highest intensity of the biharmonic pumping in the cell was 0.03 GW cm^{-2}, which corresponded to an intensity that was more than three times lower than the threshold intensity of SLFRS excitation by single-frequency radiation. If there are two spectral components in the spectrum of radiation entering the cell, then an anti-Stokes component appears in the spectrum of radiation emanating from the cell. At the highest pump energy, three Stokes and two anti-Stokes SLFRS components were recorded. The high efficiency of anti-Stokes component generation is due to the formation of a coherent dipole moment in the bulk of the active medium by biharmonic pumping.

To demonstrate the resonance nature of the interaction of biharmonic pumping with a system of submicron particles, we used a set of synthetic opal matrices as a source of two-frequency radiation with different difference frequencies. In synthetic opal matrices, SLFRS is highly efficient [34]. The frequency shift of the SLFRS is mainly determined by the size of the quartz globules that make up the matrix of synthetic opal and is in the gigahertz range. The main characteristics of the SLFRS excited in opal samples, which was obtained with the setup schematised in Fig. 1, are given in Table 3.

Table 3. Parameters of forward SLFRS.

Sample number	Average particle size/nm	SLFRS frequency shift/cm^{-1}	Highest conversion efficiency (%)	Excitation threshold/ GW cm^{-2}
1	315	0.17	55	0.11
2	290	0.22	50	0.12
3	270	0.26	50	0.14
4	245	0.37	43	0.15

Synthetic opal matrices were impregnated with ethanol and used as a source of biharmonic pumping for the excitation of SLFRS in an oil-in-water emulsion. In these cases, the difference frequency did not coincide with the acoustic eigenfrequency of the emulsion particles. The anti-Stokes component was not excited in the entire intensity range of the laser radiation used. Therefore, the interaction of a biharmonic pump with a system whose acoustic oscillation eigenfrequency coincides with the difference frequency of the pump radiation leads to efficient generation of the anti-Stokes SLFRS component.

The physical mechanism that ensures the effective influence of biharmonic pumping on the systems under study is the ponderomotive interaction. As is well known, a dielectric nanoparticle in an electric field acquires a dipole moment

$$\boldsymbol{p} = \frac{n^2 - 1}{n^2 + 2} R^3 \boldsymbol{E}_{\text{loc}}, \tag{3}$$

where $n = n_2/n_1$; n_1 is the refractive index of the environment; n_2 is the refractive index of the nanoparticle; R is the nanoparticle radius; and E_{loc} is the electric field acting on the nanoparticle. The ponderomotive force resulting from the action of an electromagnetic field on a particle is of the following form:

$$\boldsymbol{F} = (\boldsymbol{p}\nabla)\boldsymbol{E}. \tag{4}$$

If the electromagnetic field $\boldsymbol{E}$ incident on the particle consists of two waves, $\boldsymbol{E}_1$ and $\boldsymbol{E}_2$, with a frequency difference Ω and can be represented as

$$\boldsymbol{E} = \frac{1}{2}\boldsymbol{E}_1 \exp(\mathrm{i}\omega t) + \frac{1}{2}\boldsymbol{E}_2 \exp[\mathrm{i}(\omega - \Omega)t], \tag{5}$$

then there arises a component of the ponderomotive force oscillating at the frequency Ω

$$F \approx E_1 E_2 \exp(\mathrm{i}\Omega t), \tag{6}$$

which will act on the particle and excite harmonic acoustic oscillations. When the frequency Ω coincides with the particle's acoustic vibration eigenfrequency, the process acquires a resonance character.

SLFRS, which leads to coherent acoustic excitation of a system of nanosized or submicron particles in the terahertz or gigahertz frequency range, can be used to experimentally implement the generation of pulsed microwave electromagnetic radiation in nanosized and submicron systems under optical pumping, as shown in Ref. [35]. If a synthetic opal matrix acts as an active SLFRS system, then the siloxane bonds between quartz globules are broken as a result of vibrations and a charge is formed on their surface. In addition, polarisation of globules is possible due to their deformation during vibrations in asymmetric modes. The formation of charges oscillating with the vibration eigenfrequency of the particles should lead to the generation of radiation at the vibration frequency, i.e., in the gigahertz frequency range. To experimentally determine the acoustic vibration eigenfrequencies of the globules forming synthetic opal matrices, a setup comprising a nanosecond ruby laser was used (Fig. 1). The values of acoustic frequencies were determined from the spectral shift of the Stokes components of the SLFRS. In experiments on the SLFRS excited in opal matrices, spectral components were observed corresponding to the quartz-globule vibration eigenfrequencies of 16.5 and 11.4 GHz. In addition to these spectral components, we also observed compo-

nents with frequencies up to 0.75 and 1.5 GHz, which arise due to the presence of contacts between quartz globules in the opal matrix. The frequency shifts present in the SLFRS spectra agree with the results of theoretical calculations by the Lamb method and with the results of modelling by the finite element method. Figure 4 shows the results of acoustic frequency calculations for the opal matrix performed with the inclusion of siloxane bonds.

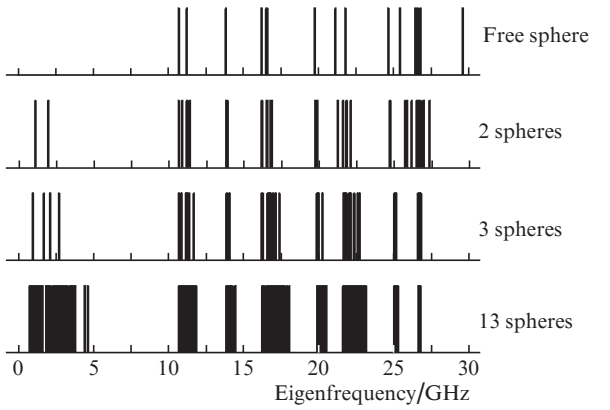

Figure 4. Acoustic eigenfrequencies calculated for 1, 2, 3 and 13 globules in contact.

To investigate the generation of electromagnetic radiation in the microwave range under optical pumping, we used a setup based on a Ti:sapphire femtosecond laser (pulse duration: 35 fs; highest pulse energy: 50 mJ; pulse repetition rate: 10 Hz; and wavelength: 800 nm). Microwave radiation was recorded using a broadband horn antenna connected to a spectrum analyser with a frequency range of up to 40 GHz (or a helical antenna connected to an oscilloscope with a frequency band of 4 GHz).

When opal matrices were pumped by ultrashort laser pulses, in the gigahertz range we recorded microwave radiation spectra, which are an array of spectral lines, the most intense of which had frequencies coinciding with the frequencies obtained in experiments on SLFRS in these systems, namely: 16.5, 11.4, 1.5 and 0.75 GHz. If bulk quartz is used instead of an opal matrix, then a uniform background without pronounced lines is observed in the microwave spectrum. Therefore, the generation of microwave radiation in submicron systems at frequencies coinciding with the acoustic eigenfrequencies of submicron particles has been experimentally demonstrated.

3. Conclusions

The paper provides a brief review of the work carried out in the G.S. Landsberg Optical Department of the P.N. Lebedev Physical Institute on the study of the SLRC in the systems of submicron and nanosized particles of various physical nature. It was shown that the SLRC can be used both to determine the morphology of the systems under study and as a source of biharmonic (two-frequency) pumping. It has also been demonstrated that the coherent excitation of a system of dielectric submicron particles, which is realised under optical pumping, can lead to the generation of electromagnetic radiation at frequencies corresponding to the natural acoustic vibration frequencies of the system used.

References

1. Landau L.D., Lifshits E.M. *Electrodynamics of Continuous Media* (Oxford: Pergamon Press, 1960; Moscow: Gostekhizdat, 1957).
2. Askar'yan G.A. *JETP Lett*., **6** (5), 157 (1967) [*Pis'ma Zh. Eksp. Teor. Fiz*., **6** (5), 672 (1967)].
3. Bykovskii Yu.A., Manykin E.A., Nakhutin I.E., Rubezhnyi Yu.G. *Sov. J. Quantum Electron*., **5**, 979 (1975) [*Kvantovaya Elektron*., **2**, 1803 (1975)].
4. Duval E., Boukenter A., Champagnon B. *Phys. Rev. Lett*., **56**, 2052 (1986).
5. Lamb H. *Proc. London Math. Soc*., **13**, 189 (1882).
6. Flugge S. *Ann. Phys.*, **5**, 373 (1941).
7. Dubrovskii V.A., Morochnik V.S. *Izv. Acad. Sci. USSR. Ser. Phys. Solid Earth*, **17**, 494 (1981) [*Izv. Akad. Nauk SSSR. Ser. Fiz. Zemli*, (7), 29 (1981)].
8. Saviot L., Murray D.B., Marco de Lucas M.C. *Phys. Rev. B*, **69**, 113402 (2004).
9. Duval E. *Phys. Rev. B*, **46**, 5795 (1992).
10. Ivanda M., Hohl A., Montagna M., et al. *J. Raman Spectrosc*., **37**, 161 (2006).
11. Mattarelli M., Montagna M., Rossi F. *Phys. Rev. B*, **74**, 153412 (2006).
12. Ovsyuk N.N., Gorokhov E.B., Grishchenko V.V., Shebanin A.P. *JETP Lett*., **47** (5), 298 (1988) [*Pis'ma Zh. Eksp. Teor. Fiz*., **47** (5), 248 (1988)].
13. Portales H., Saviot L., Duval E., Gaudry M., Cottancin E., Pellarin M., Lermé J., Broyer M. *Phys. Rev. B*, **65** (16), 165422 (2002).
14. Montagna M. *Phys. Rev. B*, **77**, 045418 (2008).
15. Gorelik V.S., Kudryavtseva A.D., Chernega N.V. *Kratk. Soobshch. Fiz. FIAN*, (8), 43 (2006).
16. Esakov A.A., Gorelik V.S., Kudryavtseva A.D., Tareeva M.V., Tcherniega N.V. *Proc. SPIE*, **6369**, 6369 OE1 (2006).
17. Trofimov V.A., Fedotov M.V., Volkov A.G., Tcherniega N.V., Savranskii V.V., Lan S. *Laser Phys*., **20**, 1137 (2010).
18. Kuok M.H., Lim H.S., Ng S.C., Liu N.N., Wang Z.K. *Phys. Rev. Lett*., **90** (25), 255502 (2003).
19. Al'mokhamed Ya., Baril' R., Vodchits A.I., Voinov Yu.P., Gorelik V.S., Kudryavtseva A.D., Orlovich V.A., Chernega N.V. *JETP Lett*., **101**, 365 (2015) [*Pis'ma Zh. Eksp. Teor. Fiz*., **101**, 399 (2015)].
20. Tcherniega N.V., Samoylovich M.I., Kudryavtseva A.D., Belyanin A.F., Pashchenko P.V., Dzbanovski N.N. *Opt. Lett*., **35** (3), 300 (2010).
21. Burkhanov I.S., Krivokhizha S.V., Chaikov L.L. *Opt. Commun*., **381**, 360 (2016).
22. Burkhanov I.S., Krivokhizha S.V., Chaikov L.L. *Quantum Electron*., **46** (6), 548 (2016) [*Kvantovaya Elektron*., **46** (6), 548 (2016)].
23. Tcherniega N.V., Zemskov K.I., Savranskii V.V., Kudryavtseva A.D., Olenin A.Yu., Lisichkin G.V. *Opt. Lett*., **38** (6), 824 (2013).
24. Ehrlich H., Kudryavtseva A., Lisichkin G., Savranskii V., Tcherniega N., Zemskov K., Zhilenko M. *Int. J. Thermophys*., **36**, 2784 (2015).
25. Burkhanov I.S., Chaikov L.L., Korobov D.Yu., Krivokhizha S.V., Kudryavtseva A.D., Savranskiy V.V., Shevchuk A.S., Tcherniega N.V. *J. Russ. Laser Res*., **33**, 496 (2012).
26. Averyushkin A.S., Baranov A.N., Bulychev N.A., Kazaryan M.A., Kudryavtseva A.D., Strokov M.A., Tcherniega N.V., Zemskov K.I. *Opt. Commun*., **389**, 51 (2017).
27. Ehrlich H.V., Kudryavtseva A.D., Lisichkin G.V., Mironova T.V., Savranskii V.V., Tcherniega N.V., Zemskov K.I., Zhilenko M.P. *J. Russ. Laser Res*., **37** (3), 291 (2016).
28. Gorelik V.S., Tcherniega N.V., Shevchenko M.A., Pyatyshev A.Yu., Umanskaya S.F., Voropinov A.V., Bi D. *Soft Matter*, **16**, 8848 (2020).
29. Tcherniega N.V., Pershin S.M., Bunkin A.F., Donchenko E.K., Karpova O.V., Kudryavtseva A.D., Lednev V.N., Mironova T.V., Shevchenko M.A., Strokov M.A., Zemskov K.I. *Laser Phys. Lett*., **15**, 095603 (2018).

30. Arkhipenko M.V., Bunkin A.F., Davydov M.A., Karpova O.V., Oshurko V.B., Pershin S.M., Strel'tsov V.N., Fedorov A.N. *JETP Lett*., **109**, 578 (2019) [*Pis'ma Zh. Eksp. Teor. Fiz*., **109** (9), 598 (2019)].
31. Karpova O.V., Arkhipenko M.V., Pershin S.M., Karpov M.A., Kudryavtseva A.D., Mironova T.V., Savichev V.I., Shevchenko M.A., Tcherniega N.V., Umanskaya S.F. *J. Russ. Laser Res*., **42** (1), 106 (2021).
32. Chernega N.V., Kudryavtseva A.D., Samoilovich M.I., Shevchuk A.S., Kleshcheva S.M. *Optoelectron., Instrum. Data Proces*., **48**, 1 (2012) [*Avtometriya*, **48** (3), 39 (2012)].
33. Shevchenko M.A., Chaikov L.L., Tcherniega N.V. *Spectrochim. Acta. Part A: Mol. Biomol. Spectrosc*., **245**, 118902 (2021).
34. Kudryavtseva A.D., Tcherniega N.V., Samoylovich M.I., Shevchuk A.S. *Int. J. Thermophys*., **33** (10), 2194 (2012).
35. Shevchenko M.A., Karpov M.A., Kudryavtseva A.D., Rozinskii D.V., Tcherniega N.V., Umanskaya S.F. *Sci. Rep*., **11**, 7682 (2021).